

ORIGINAL RESEARCH REPORT

Targeted delivery of paclitaxel by NL2 peptide-functionalized on core-shell LaVO₄:Eu³⁺@ poly (levodopa) luminescent nanoparticles

Hamid Hashemi-Moghaddam¹ | Mansore Ebrahimi¹ | Behrooz Johari² |
Hamid Madanchi^{3,4}

¹Department of Chemistry, Damghan Branch, Islamic Azad University, Damghan, Iran

²Department of Medical Biotechnology, School of Medicine, Zanjan University of Medical Sciences, Zanjan, Iran

³Department of Biotechnology, School of Medicine, Semnan University of Medical Sciences, Semnan, Iran

⁴Drug Design and Bioinformatics Unit, Department of Medical Biotechnology, Biotechnology Research Center, Pasteur Institute of Iran, Tehran, Iran

Correspondence

Hamid Madanchi, Department of Biotechnology, School of Medicine, Semnan University of Medical Sciences, Semnan, Iran.
Email: hamidmadanchi@yahoo.com

Abstract

Targeted drug delivery enhances drug efficiency and selectivity without affecting normal cells. Luminescent nanoparticles can be used for tumor imaging as well as selective tumor targeting for drug delivery. In this research, LaVO₄:Eu³⁺ was synthesized, the luminescent nanocrystal was coated by surface polymerization of levodopa in the presence of Paclitaxel (PTX), and then NL2 peptide was coupled on the surface of polymer-coated luminescent nanoparticles. Next, the capability of the modified drug was examined by in vitro and in vivo experiments. MTT assay on SK-BR-3 cell line (as breast cancer cells) and fluorescent microscopy results indicate that this modification decreases significantly drug toxicity and increases its selectivity. In addition, in vivo experiments confirm more capability of the NL2-functionalized nanocomposite for reducing tumor size, drug distribution in the body, and more aggregation of PTX in tumor tissue. Overall, it is concluded that tumor imaging is possible using luminescent LaVO₄:Eu³⁺ core and NL2 peptide increases significantly the specificity of PTX in combination with a functionalized luminescent polymeric carrier.

KEYWORDS

breast cancer, levodopa, luminescent nanoparticles, paclitaxel, tumor-targeted peptides

1 | INTRODUCTION

The luminescent nanomaterials have several potential applications in medicine and pharmaceuticals for example in bio-labeling and drug targeting,¹⁻³ diagnostic analysis,^{4,5} fluorescent and optical bio-probes,⁶ and drug delivery carriers.⁷ Nanomaterials with luminescent properties such as quantum dots, metals,⁸ and lanthanide⁹ organic dyes¹⁰ are extensively used in biological studies. Among these materials, rare-earth-doped nanoparticles reveal several advantages such as great photostability and chemical stability and have been broadly used in the area of luminescent analysis¹¹ in vivo/vitro imaging.^{12,13} However, surface modification of the particles is a sensitive step for biological applications. This process is applied to increase their biocompatibility and water solubility, as well as reducing their toxicity.

Polydopamine (PDA) is one of the best coatings for nanoparticles because it can be directly polymerized through a biocompatible and stable layer.¹⁴⁻¹⁶ In this way, a very thin coated layer is formed that is crucial in biological applications. The carboxylic groups in the synthesized polymer are highly hydrophilic and can advance the spread of luminescent polymeric carriers in a biological system.¹⁶ Moreover, it has negligible side effects and does not show immunogenicity. Easy polymerization condition is another important advantage of dopamine and sensitive drugs could be encapsulated.¹⁷

Among targeting ligands, peptides have increasingly attracted tumor diagnostics and therapeutics because of their advantages such as high affinity, small sizes, stability, low immunogenicity, and ease of modification. Moreover, peptides are noticeably smaller than mAbs and do not interact with the reticuloendothelial system.^{18,19}

Therefore, peptides have been recently developed in new fields such as tumor-targeting agents for imaging or therapeutic goals.²⁰⁻²³ Another example of using these molecules is coupling tumor-targeting peptides to the synthesized luminescent polymeric carrier to enhance their tumor selectivity.²²

NL2 peptide (AEGEFIHNRYNRFFYWYGDPK) is a tumor-targeting peptide that was first synthesized by the T7 phage library.²⁴ Also, previous studies have shown that NL2 peptide has good stability and tumor targeting activity with a specific diagnosis of HER2 tumor marker without toxicity.^{25,26} Human epidermal growth factor receptor 2 (HER2) is known as a tumor marker that is over-expressed on more than 30% of breast cancers (HER2, c-erbB2)^B.

In the present study, levodopa was polymerized on the surface of synthesized LaVO₄:Eu³⁺ nanocrystals in the presence of paclitaxel (PTX) as an anticancer drug. Next, NL2 peptide was coupled on polymer-coated nanocrystals and the performance of the prepared system was investigated in comparison with that of the non-functionalized luminescent polymeric carrier.

2 | MATERIALS AND METHODS

2.1 | Materials, media, cell line, and animals

Levodopa, Streptomycin, Penicillin, and Cyclosporin as antibiotics of cell culture, Trepan, Trypsin, blue dye, dimethyl sulfoxide (DMSO), MTT dye (3-[4, 5-dimethylthiazol-2-yl]-2, 5-diphenyltetrazolium bromide), PTX, La(NO₃)₃·6H₂O, and Eu(NO₃)₃·6H₂O (purity>99.9%) were obtained from Sigma Company (Sigma-Aldrich, MO). Other used chemicals were purchased from Merck (Darmstadt, Germany). To evaluate NL2 tumor recognizing activity at in vitro and in vivo assay, SK-BR-3 cell line NCBI code C207 (National Cell Bank of Iran, Pasture Institute of Iran) was applied as HER2 positive breast cancer cell for cytotoxicity test. Fetal bovine serum (FBS) and Roswell Park Memorial Institute medium (RPMI) 1,640 medium were purchased from Gibco Company (Gibco, Carlsbad, CA). For the animal study, forty 6-8-week C57BL/6 nude mice were purchased from the Pasteur Institute of Iran.

2.2 | Synthesis and functionalization of the luminescent polymeric carrier

2.2.1 | Synthesis of NL2 peptide

NL2 peptide (a tumor-targeting peptide that recognizes HER2/neu tumor marker) was selected based on our previous study.²² This peptide (H-AEGEFIHNRYNRFFYWYGDPK-OH) was synthesized commercially. The solid-phase method was used for the synthesis of NL2 peptide based on fluorene-9-methoxycarbonyl (Fmoc)-polypeptide active ester chemistry.²⁷ synthesis was carried out by Mimotopes Pty Ltd (Clayton, Victoria, Australia). Mass spectrometry (Sciex API100 LC/MS mass spectrometer; Perkin Elm Co., Norwalk, CT) and

RP-HPLC were used to determine molecular weights and purity of NL2 peptide.

2.2.2 | Synthesis of luminescent nanoparticles

First, sodium orthovanadate (Na₃VO₄) was prepared by adding 0.6 g NaOH to 0.06 g NH₄VO₃. Then, a mixture of 20 μl of Europium nitrate (Eu(NO₃)₃·6H₂O) and 980 μl La(NO₃)₃·6H₂O (both 1.0 mol/L) was poured into 10 ml distilled water and was added drop-wise into the Na₃VO₄ solution at 80°C and kept under constant stirring for 2 hr. Then, the pH value was adjusted to 8-9 by aqueous ammonia. Subsequently, the solution was centrifuged and the precipitate sample collected. Next, it was washed with absolute ethanol and distilled water three times and dried in the oven at 200°C for 6 hr.²⁸

2.2.3 | Surface polymerization of luminescent LaVO₄:Eu³⁺ NPs and evaluation of the PTX loading capacity in it

For polymer coating of luminescent nanoparticles, LaVO₄:Eu³⁺ nanoparticles (0.5 g) were added to 150 ml of Tris buffer (10 mM, pH 8.5). Afterward, levodopa (0.5 g) and PTX (250 mg) were added to the solution and stirred mechanically for 14 hr at room temperature. The resulting sample was centrifuged and then was spread into the water and kept at 4°C. To evaluate the capacity of luminescent LaVO₄:Eu³⁺ NPs for PTX loading, PTX concentration at t₂ (at the moment of PTX addition) and t₁ (after 14 hr) was calculated from the absorption at 230 nm in solution in relation to a standard calibration curve (absorption/concentration curve). The percentage of PTX-loaded was determined using the following equation:

$$\text{Unabsorbed PTX\%} = \frac{\text{PTX concentration in t}_1}{\text{PTX concentration in t}_0} \times 100.$$

$$\text{Loaded PTX\%} = 100 - \text{Unabsorbed PTX\%}.$$

2.2.4 | Coupling NL2 peptide to polymer-coated luminescent nanoparticles

NL2 peptide was coupled to poly(levodopa) coated luminescent nanoparticles through a two-step method described by Jiang et al.²⁹ Initially, 2.3 ml the aqueous solution of N-hydroxysuccinimide (NHS) (50 mg ml⁻¹) was added to 1 g of polymer-coated luminescent nanoparticles in 5 ml of water and stirred rapidly. Next, 1.2 ml aqueous solution of N-ethyl-N'-(3-dimethyl aminopropyl) carbodiimide hydrochloride (EDAC) (10 mg ml⁻¹) was fast added to the solution, followed by stirring the solution for 30 min while keeping the pH between 7.5 and 8. The sample was dialyzed in distilled water for

10 hr to remove its extra EDAC, NHS, and byproduct urea. Subsequently, 1 ml of peptide solution (1 mg ml⁻¹) was added to 1 g of the esterified polymer in 14 ml of water and mixed 24 hr. Finally, the unbound peptide was removed by dialysis of the sample in distilled water for 72 hr.

2.3 | Luminescent polymeric carrier characterization

2.3.1 | Surface analysis by SEM

Field-emission scanning electron microscopy (FESEM; VEGA, TESCAN, Brno, Czech Republic) was used to assess the surface morphology and sizes of the NC-PTX in accordance with the standard protocol.³⁰

2.3.2 | Fourier transforms infrared spectra

Chemical structure of synthesized peptide-functionalized luminescent nanocomposite was assessed using a 6,700 Thermo Nicolet Fourier transform infrared (FTIR) spectroscopy by the KBr pellet method at a range of 400–4,000 cm⁻¹.

2.3.3 | XRD pattern

The crystalline structure of synthesized nanocomposite was confirmed by X-ray diffraction (Bruker-D8 XRD) with Cu K α radiation ($k = 1.5418 \text{ \AA}$) operating at 40 kV and 30 mA. Scherrer formula was used for calculating the diameter of the synthesized nanoparticles.^{31,32}

2.3.4 | Fluorescence measurements

Fluorescence measurements were carried out using a JASCOFP-6500 spectrophotometer equipped with a xenon discharge lamp (150 W) LaVO4: Eu3@ poly (levodopa). Luminescent nanoparticles spectra were prepared through subsequent scanning emission spectra from 550 to 710 nm at 2 nm increments by the excitation wavelength from 280.

2.4 | In vitro experiments

2.4.1 | Evaluation of in vitro PTX release

A Varian (Cary100, Australia) UV-Vis spectrophotometer was used for evaluating the PTX release pattern from luminescent nanocomposite. First, PTX was loaded on a nanocomposite and then PTX release was evaluated at 37°C and pH = 7.4. Finally, absorption was measured at 230.0 nm.

2.4.2 | Investigating the anticancer activity of nanocomposite functionalized by NL2 peptide by cytotoxicity assay

MTT assay was used to determine the toxicity of the luminescent nanocomposite without PTX (NC) and luminescent nanocomposite with PTX and NL2 peptide (NC-PTX). SK-BR-3 cell line was cultured at 1×10^5 cells/well for 24 hr under optimal conditions (i.e., 37°C, 5% CO₂ in a humidified incubator). Then, the cells were washed two times with PBS, and the growth medium was removed. New maintenance RPMI (Gibco, Carlsbad, CA) medium containing 2.5, 5, 10, 20, and 30 $\mu\text{g ml}^{-1}$ of each compound were incubated for 24, 48, and 72 hr.³³ Quintet wells were analyzed for each concentration and PBS was used as a control. Besides, commercial PTX was used as a positive control. A 10 μl solution of 5 mg ml⁻¹ MTT in PBS was added to each well and incubated for 4 hr. Next, the media was removed and 100 μl isopropanol was added to the well. Plates were shaken smoothly. A microplate reader (STAT FAX 2100, USA) was used at 545 nm.

2.4.3 | Evaluating the selectivity of nanocomposite with and without NL2 peptide

The selectivity of NL2 peptide for HER2 positive cells was determined using fluorescent microscopy. For this purpose, the SK-BR-3 cell line was cultured at 50×10^5 cell/well in 6-well plates for 24 hr at optimized conditions (i.e., 37°C, 5% CO₂ in a humidified incubator). Then, the medium was removed and the cells were washed in triplicate with PBS. Next, new maintenance RPMI (Gibco, Carlsbad, CA) medium (10% FBS) containing functionalized and unfunctionalized NL2 nanocomposite (with and without NL2 peptide, respectively) at 20 $\mu\text{g ml}^{-1}$ concentration was added to cells and incubated for 4 hr. After the incubation, the respective medium was discarded and cells were washed three times with PBS (300 μl) to remove unbound nanocrystals-PTX. These cells were then fixed on the slip using 4% paraformaldehyde and glycerin/PBS solution. Next, to evaluate the binding of nanocomposite that was functionalized with NL2 peptide, cells were observed by fluorescence microscopy at 700 nm for excitation (Leica TCS SP5 II laser scanning confocal microscope, Leica microsystem Inc.,IL) (Wang et al., 2013).

2.5 | In vivo investigation

2.5.1 | Animals ethics statement

Forty adult female C57BL/6 nudes (6–8 weeks) were purchased from Pasteur Institute of Iran. The mice were maintained under normal standard conditions, that is, 12 hr of darkness and 12 hr of light. Animal experiments in this study were carried out according to the declaration of Helsinki as revised in Tokyo 2004 and the protocol of Islamic Azad University, Damghan Branch (23–332).

2.5.2 | Human tumor cells xenograft

First, 200 μl of SKBR3 cells at a total concentration of $4 \times 10^7/\text{ml}$ were injected into the flank region of anesthetized nude mice using a 29-gage syringe needle. To anesthetize the mice, xylazine, and ketamine (10 and 100 mg/kg/BW, respectively) were injected intraperitoneally (i.p). Tumor sizes were measured daily until they reached 10 mm³. Mice bearing tumors were randomly divided into control group (without any treatment) or treatment groups (n = 10 mice/group) and treated simultaneously. Treatment groups included commercial drug (PTX), nanocomposite without NL2 peptide (NC), and peptide-functionalized nanocomposite with NL2 peptide (NCP or NC-PTX).

The tumor-bearing mice correspondingly received 5 mg/kg/BW of PTX from commercial PTX, NC, and NCP dissolved in distilled water intravenously via the tail vein.

2.5.3 | Tumor sizes measurement and survival rates

Tumor dimensions were identified in three dimensions of length, width, and height by the caliper. Next, tumor volume and body weights were measured until the 25th day after treatment in 5-day intervals. Tumor volume (V) was obtained as described in the previous study.¹⁶

2.5.4 | Determination of PTX distribution in various tissues

PTX concentration in liver, heart, kidney, and tumor tissue was determined by HPLC as previously reported¹⁶ (Reversed-Phase; A Knauer D-14163; Berlin, Germany). HPLC instrument was used for PTX identification. Moreover, the integration of chromatograms was calculated by a Knauer EZChrom software package.

2.6 | Statistical analysis

Statistical analysis was carried out by one-way analysis of variance (ANOVA) and Tukey's HSD as post hoc test using SPSS Statistics 22.0 software (SPSS Inc. Chicago, IL). The *p* values of <.05 were considered as statistically significant.

3 | RESULTS

3.1 | Characterization of peptide-functionalized luminescent nanocomposite

3.1.1 | Surface characterization

The morphology of the NC-PTX was examined by SEM. It is of note that luminescent nanocomposite is relatively monodisperse with an average diameter of roughly 51.5 ± 9.4 nm (Figure 1).

3.1.2 | FTIR spectra

The FTIR spectra of the synthesized LaVO₄:Eu³⁺ and polymer-coated luminescent nanocomposite were evaluated by FTIR spectroscopy. The main absorption band of the V—O (from the VO₄³⁻ group) appeared at 804 cm⁻¹. Also, a weak band was seen at 439 cm⁻¹, which is attributed to La (Ln)—O bond. These results confirm the presence of the crystalline LaVO₄ phase.²⁸

Moreover, FTIR spectra were recorded after the surface coating of LaVO₄:Eu³⁺ nanoparticles by polymerization of levodopa. FTIR spectra show the —OH and —NH groups show a broad absorbance band at 3,418 cm⁻¹. The aromatic rings in the poly(levodopa) are confirmed by a weak peak at 1610 cm⁻¹. Peaks at 1,515 and 1,605 cm⁻¹ are consistent with the indole or indoline structures. A large broad peak spanning appeared at 3,200–3,500 cm⁻¹ is attributed to the presence of —OH and —NH structures. No carbonyl structures were discernible from this analysis; however, these absorbances might be obscured by the broad peak observed between 800 and 1,710 cm⁻¹ (Figure 2).

3.1.3 | XRD pattern

The crystalline structure of the synthesized LaVO₄:Eu³⁺ was examined by XRD (Figure 3). The XRD pattern assessment shows that the synthesized sample is crystalline and literature data confirm diffraction peaks for crystalline LaVO₄:Eu₃.²⁸ There are no trace impurity peaks in the XRD pattern, confirming the single-phase tetragonal zircon type of synthesized LaVO₄ luminescent nanoparticles.

3.1.4 | Photoluminescence properties

The photoluminescence measurement revealed that the luminescent properties of the samples change by varying their morphologies.³⁴ The photoluminescence properties of the polymer-coated LaVO₄:Eu³⁺

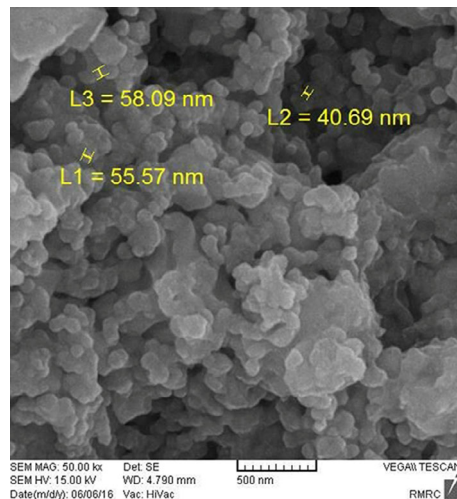


FIGURE 1 SEM images of functionalized nanocomposite

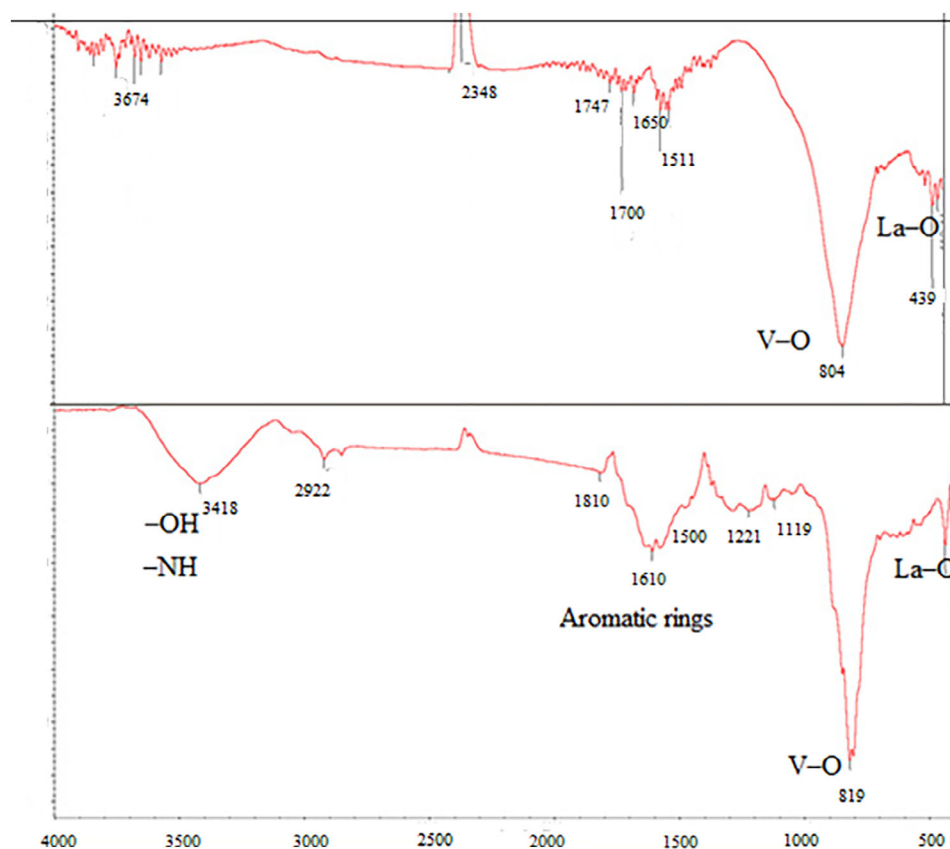


FIGURE 2 FTIR spectrum of the synthesized nanocomposite. (a) $\text{LaVO}_4:\text{Eu}^{3+}$ nanoparticles and (b) NL2 functionalized polymer coated $\text{LaVO}_4:\text{Eu}^{3+}$ nanoparticles. FTIR, Fourier transform infrared

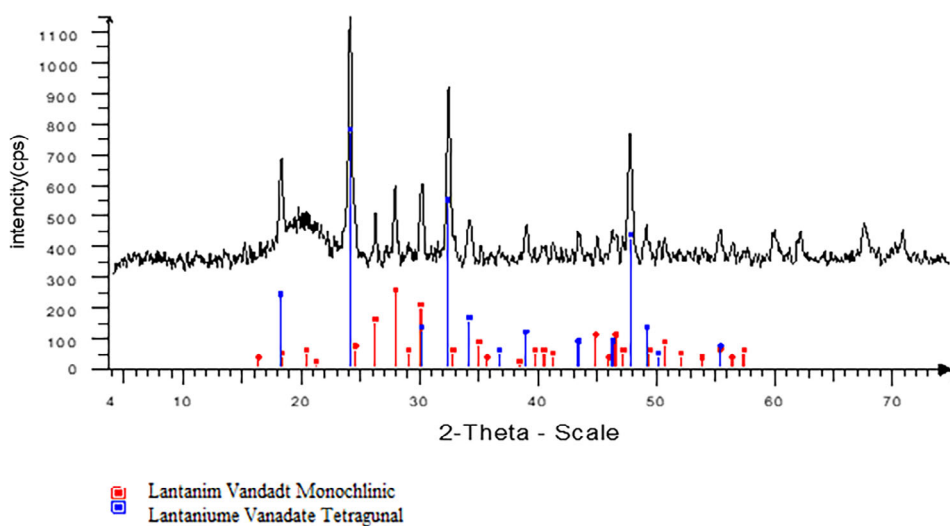


FIGURE 3 XRD pattern of synthesized $\text{LaVO}_4:\text{Eu}^{3+}$. XRD, X-ray diffraction

nanocomposite were investigated by the fluorescence spectrometer at an excitation wavelength of 280 nm. Spectral transitions were recorded in the range from 550 to 740 nm, which are related to the transitions from the excitation levels of $5D_0$ to $7F_J$ ($J = 1, 2, 3,$ and 4) of the Eu^{3+} activators. The strongest emission is the $5D_0/7F_2$ transition, which appeared in the range of 600–630 nm. This peak is

attributed to the red emission, which is in good agreement with the Judd-Ofelt theory.^{35–37} Here, no emission was identified from transitions from VO_4^{3-} groups. The sharp peak in the red region emanating from the $5D_0/7F_2$ (620 nm) transition can be attributed to the low-local symmetry (D_{2d}) for the sites of Eu^{3+} in the LaVO_4 host lattices. The photoluminescence spectra are shown in Figure 4.

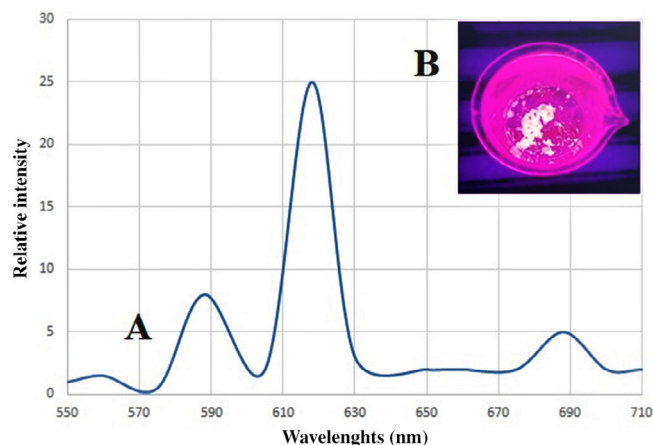


FIGURE 4 Photoluminescence spectrum of the NL2 functionalized luminescent nanocomposite

3.2 | In vitro experiments

3.2.1 | Assessment of in vitro PTX loading and release kinetics

The average maximum adsorption capacity was $73.4 \mu\text{mol g}^{-1}$ for three measurements. Therefore, it can be stated that 25.07% of the initial concentration of the PTX is absorbed per gram of nanoparticles.

For PTX release investigation, first, 25 mg of PTX was loaded on 1 g of the luminescent nanocomposite, followed by investigating its release was investigated in the dialysis bag by determining its released PTX. The luminescent nanocomposite release gently PTX, the PTX release was stopped after 22 hr. The results of this experiment revealed a relatively slow release rate until 24 hr. Thus, a constant PTX delivery to the tumor could be attained by the synthesized nanoparticle. The PTX release pattern is illustrated in Figure 5.

3.2.2 | MMT assay results

The toxicity of nanoparticle components without PTX (NC) and with the PTX after the release from nanoparticle with PTX (NC-PTX) was performed using free PTX and MTT assay on SK-BR-3. Figure 6a presents MTT assay results on the SK-BR-3 cell line for the luminescent nanoparticle without PTX (NC), nanoparticle with PTX (NC-PTX), and commercial PTX. The results showed that NC had 1 to 3.5% toxicity in the concentration of $2.5\text{--}30 \mu\text{g ml}^{-1}$. This particle compared with NC-PTX was found to be non-toxic for the cancer cell line. Also, NC was identified as a good and nontoxic vehicle for the delivery of PTX. NC-PTX showed the toxicity of about 14–78% at $2.5\text{--}30 \mu\text{g ml}^{-1}$. The toxicity of PTX at $2.5\text{--}30 \mu\text{g ml}^{-1}$ was about 31–79%. Therefore, NC-PTX retains PTX toxicity in three time intervals. Also, NC-PTX toxicity at different time intervals (24, 48, and 72 hr) showed that PTX release is controlled by this particle. For example, the toxicity level of $30 \mu\text{g ml}^{-1}$ of NC-PTX was 63% after 24 hr, while this amount increased to 78% after 72 hr. It is of note that the concentration of PTX in the NC-PTX groups

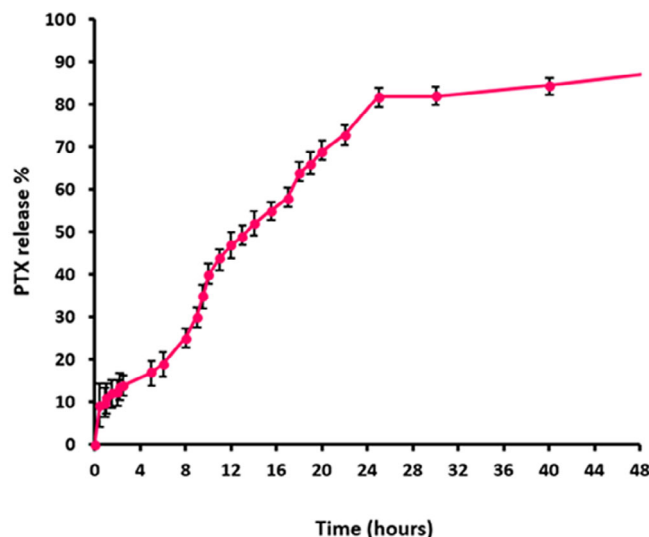


FIGURE 5 The pattern of PTX release from luminescent nanocomposite. PTX, paclitaxel

is low due to the limited drug loading capacity in NC. Therefore, similar lethal effects with the PTX group may be seen. In addition to the PTX toxicity, NC, NL2 peptide, and nutrient deficiency caused inhibition of cell growth. In the first 24 hr, at a concentration of $30 \mu\text{g m}^{-1}$, the free PTX killed 79% of the cells while this amount is 63% for NC-PTX. This value is significantly less than that of free PTX because there is a less real concentration of PTX in NC-PTX, while the concentration mentioned about free PTX is more realistic.

3.2.3 | The selectivity determination of NL₂ functionalized and nonfunctionalized luminescent nanoparticle

The results of cell imaging by laser scanning confocal microscope indicated that NL₂ functionalized luminescent nanoparticles can recognize SK-BR-3 cell line and attach to them. The reason is that after washing, it is also retained on the cells' surface. However, a nonfunctionalized luminescent nanoparticle that lacks NL₂ peptide after washing was not observed on the cells' surface (Figure 7a,b). Images indicated that NL₂ functionalized luminescent nanoparticle is selective nanoparticle for HER2 protein while nonfunctionalized luminescent nanoparticle has no selectivity for HER2 positive cells. Therefore, it can be suggested that NL₂ peptide-functionalized poly-levodopa coated LaVO₄:Eu³⁺ + luminescent nanocrystals can be recognized specifically in HER2 positive cells.

3.3 | In vivo experiments

3.3.1 | Investigating the NL₂ functionalized luminescent nanoparticle on tumor growth

Effects of different types of PTX in commercial form and modified forms were investigated on tumor growth in nude mice. The obtained

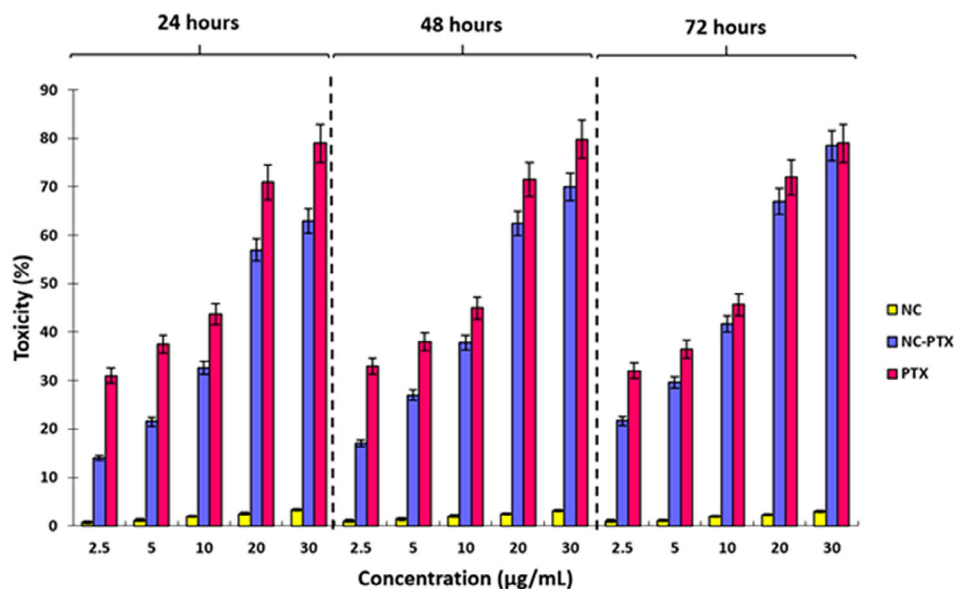


FIGURE 6 The percentage of toxicity of NC-PTX, NC, and commercial PTX after (a) 24 hr, (b) 48 hr, and (c) 72 hr. Error bars indicate SD. PTX, paclitaxel

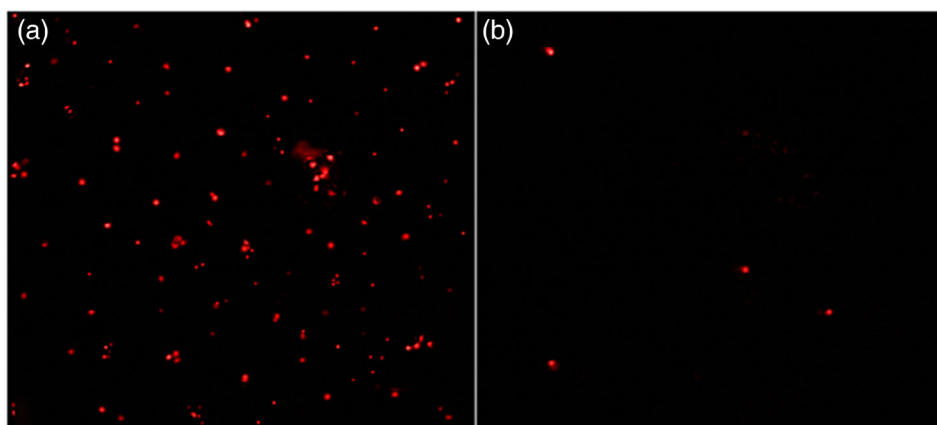


FIGURE 7 The laser scanning confocal microscope image after incubation with $20 \mu\text{g ml}^{-1}$ of (a) NL2 functionalized luminescent nanocomposite and (b) nonfunctionalized luminescent nanocomposite

results showed that tumor volume declined significantly in the NCP group compared to nonmodified PTX ($p < .05$). Mean tumor volumes after treatment at various days are presented in Figure 8

, where error bars show the standard deviation of the mean. The results show no statistically significant difference between the tumor volume of the commercial PTX and NC-PTX treated groups ($p > .05$). Nevertheless, tumor volume was significantly decreased in the treated group with commercial NC and PTX compared to the control group ($p > .05$).

3.3.2 | Distribution of PTX in different tissues

The results for treated groups with modified drugs show that PTX was deposited in the tumor of the NCP-treated group and its concentration is significantly higher than other treated groups. PTX concentrations in the liver, heart, and kidney tissues are significantly lower compared to tumor tissue in the NCP group. Moreover, the PTX concentration in the NC group is not significantly

more than commercial PTX. PTX was not detected in untreated group tissues. Figure 9 presents the concentration of PTX in different tissues.

4 | DISCUSSION

$\text{LaVO}_4:\text{Eu}^{3+}$ is a luminescent nanoparticle that can be used for tumor imaging. The peptide functionalization of polymer-coated $\text{LaVO}_4:\text{Eu}^{3+}$ nanoparticles produces a luminescent nano-drug that can be used for tumor imaging and targeting. PDA is a biocompatible polar polymer with good water solubility that can directly and easily be polymerized in ambient conditions, and have.³⁸⁻⁴¹

In this study, the MTT assay showed that NL2 functionalized nanocomposite has toxic effects similar to those of PTX alone on SK-BR-3 cells. Therefore, this nanoparticle can release all or most of the drug (PTX) effectively. Also, MTT assay results at different time intervals (24, 48, and 72 hr) show that PTX release is controlled by this nanocomposite. Imaging by confocal microscopy is a good

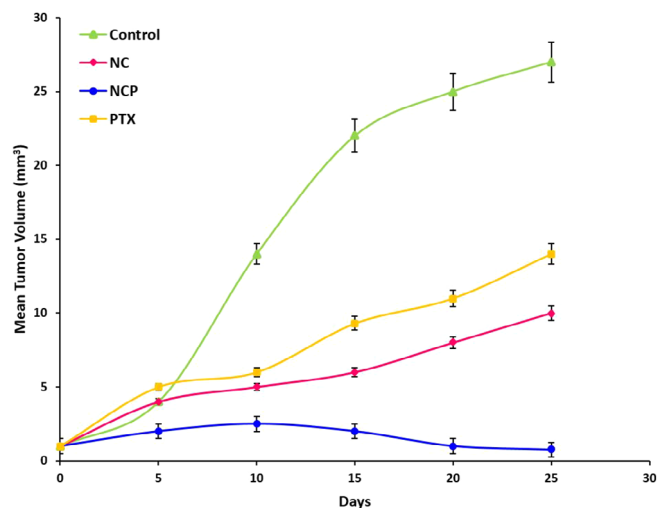


FIGURE 8 Changes in the tumor volumes after treatment with modified PTX. NC: PTC combined with nanocomposite and NCP: combined drug with nanocomposite plus peptide. PTX, paclitaxel

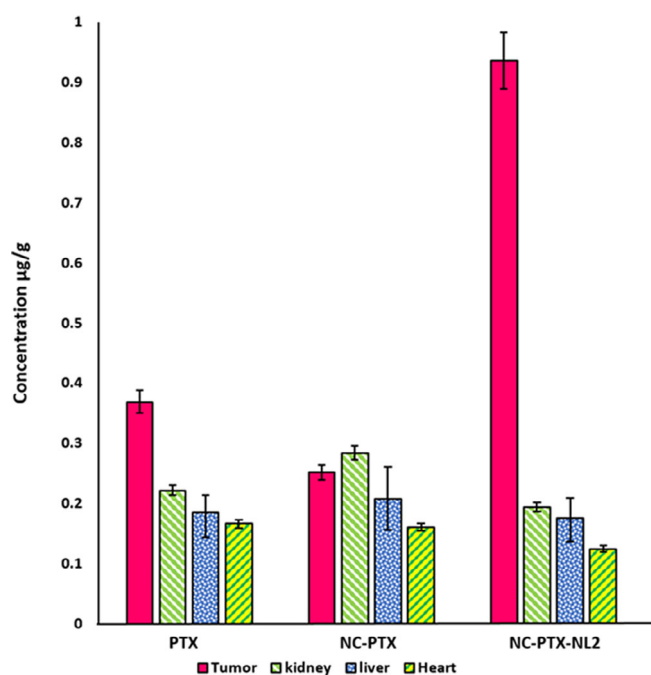


FIGURE 9 Concentration of PTX in experimental tissues groups of NC: drug in combination with nanocomposite and NCP: peptide coupled nanocomposite with plus PTX. PTX, paclitaxel

method for evaluating the luminescence labeled nanoparticles (Wang et al. 2013). The luminescence intensity in NL2-coated nanocomposite (NC-PTX) after washing the treated SK-BR-3 cells was strong, while this parameter was negligible in nanocomposite without NL2 (NC). This result indicates that NL2 peptide increases the affinity of the NC-PTX for the HER2 positive cancer cells and can help targeted drug delivery to these cells.

Assessment of the PTX release kinetics revealed that it released slowly for 24 hr. In vivo experiments of synthesized luminescent nano-drug confirms its selectivity for tumor cells. Moreover, higher PTX accumulation in tumor tissue was observed in HPLC data.

Investigating the tumor growth in different groups shows that NCP or NC-PTX treatment provides supreme tumor growth inhibition. Direct delivery of PTX to the tumor cell is a reason for the excellent selectivity of NCP and high-drug deposition in this group.

Finally, this research showed that using synthesized NL2 functionalized nano-drug increased local PTX concentration in mice bearing breast tumor, and NL2 increases the affinity of this functionalized nanoparticle for the HER2 positive cancer cells. Therefore, NL2 peptide coated-luminescent nanocomposite can be used in targeted drug delivery of PTX or other anticancer drugs to HER2 positive cells.

5 | CONCLUSION

A variety of luminescent nanoparticles have been developed and engineered for specific applications of drug imaging and delivery systems.⁴²⁻⁴⁴ Functionalization of nanomaterials increases significantly its targeting properties and leads to considerable progress in the fundamental understanding, diagnosis, and treatment of cancer. Vanadate compounds are widely used matrices for luminescent rare earth (RE) ions dopants as they satisfy the high efficiency of excitation of activator through the matrix.⁴⁵ Because of the inherent complexity of the LaVO₄: Eu³⁺ and the safety concerns, these modifications reduce toxicity, enhanced selectivity, and include the capability of tumor imaging.

ACKNOWLEDGMENT

We thank the Semnan University of Medical Sciences and Drug Design and Bioinformatics Unit of Pasteur Institute of Iran.

CONFLICT OF INTEREST

The authors declare that they have no conflict of interest.

DATA AVAILABILITY STATEMENT

The data that support the findings of this study are available from the corresponding author upon reasonable request.

REFERENCES

- Das P, Ganguly S, Mondal S, et al. Dual doped biocompatible multi-color luminescent carbon dots for bio labeling, UV-active marker and fluorescent polymer composite. *Luminescence*. 2018;33(6):1136-1145.
- Aldalbahi A, Rahaman M, Ansari AA. Mesoporous silica modified luminescent Gd²⁺O₃:Eu nanoparticles: physicochemical and luminescence properties. *J Sol-Gel Sci Technol*. 2019;89(3):785-795.
- Burunkova J, Keki S, Veniaminov A, Nagy M, Daroczi L, Kokenyesi S. Influence of gold nanoparticles on the luminescence of an acrylated isocyanonaphthalene derivative. *Adv Condensed Matter Phys*. 2019;2019:1-5.

4. Zhao Z, Zhang X, Li C-e, Chen T. Designing luminescent ruthenium prodrug for precise cancer therapy and rapid clinical diagnosis. *Biomaterials*. 2019;192:579-589.
5. Rück A, Reeß K, von Einem B, Kalinina S. Multiparametric luminescence lifetime imaging: a new diagnostic tool to follow up bioenergetic alterations during PDT. *Int Soc Opt Photonics*. 2019;1088207. 10882.
6. Dasari S, Singh S, Kumar P, Sivakumar S, Patra AK. Near-infrared excited cooperative upconversion in luminescent ytterbium (III) bioprobes as light-responsive theranostic agents. *Eur J Med Chem*. 2019;163:546-559.
7. Yao L, Hu Y, Liu Z, Ding X, Tian J, Xiao J. A luminescent lanthanide-collagen peptide framework for pH-controlled drug delivery. *Mol Pharm*. 2018;16(2), 846-855.
8. Wang H, Wang L. One-pot syntheses and cell imaging applications of poly (amino acid) coated LaVO₄: Eu³⁺ luminescent nanocrystals. *Inorg. Chem*. 2013;52(5), 2439-2445.
9. Qu X, Li Y, Li L, Wang Y, Liang J, Liang J. Fluorescent gold nanoclusters: synthesis and recent biological application. *J Nanomater*. 2015;2015:4.
10. Zhang Y, Han G. Lanthanide-doped Upconverting Nanoparticles for Biological Applications. *Perspect Micro Nanotechnol Biomed Appl: World Sci*. 2016;1, 37-64.
11. Long Z, Liu M, Jiang R, et al. Preparation of water soluble and biocompatible AIE-active fluorescent organic nanoparticles via multicomponent reaction and their biological imaging capability. *Chem Eng J*. 2017;308:527-534.
12. Zhong Y, Ma Z, Zhu S, et al. Boosting the down-shifting luminescence of rare-earth nanocrystals for biological imaging beyond 1500 nm. *Nat Commun*. 2017;8(1):737.
13. Zong L, Wang Z, Yu R. Lanthanide-doped photoluminescence hollow structures: recent advances and applications. *Small*. 2019;1804510.15(29).
14. Niu F, Yan J, Ma B, et al. Lanthanide-doped nanoparticles conjugated with an anti-CD33 antibody and a p53-activating peptide for acute myeloid leukemia therapy. *Biomaterials*. 2018;167:132-142.
15. Oroujeni M, Kaboudin B, Xia W, Jönsson P, Ossipov DA. Conjugation of cyclodextrin to magnetic Fe₃O₄ nanoparticles via polydopamine coating for drug delivery. *Prog Org Coat*. 2018;114:154-161.
16. Sahiner N, Sagbas S, Sahiner M, Blake DA, Reed WF. Polydopamine particles as nontoxic, blood compatible, antioxidant and drug delivery materials. *Colloids Surf B Biointerfaces*. 2018;172:618-626.
17. Hashemi-Moghaddam H, Zavareh S, Gazi EM, Jamili M. Assessment of novel core-shell Fe₃O₄@ poly l-DOPA nanoparticles for targeted Taxol® delivery to breast tumor in a mouse model. *Mater Sci Eng C*. 2018;93:1036-1043.
18. Hashemi-Moghaddam H, Zavareh S, Karimpour S, Madanchi H. Evaluation of molecularly imprinted polymer based on HER2 epitope for targeted drug delivery in ovarian cancer mouse model. *React Funct Polym*. 2017;121:82-90.
19. Keservani RK, Sharma AK, Jarouliya U. Protein and peptide in drug targeting and its therapeutic approach. *Ars Pharmaceutica*. 2015;56(3):165-177.
20. Aina OH, Sroka TC, Chen ML, Lam KS. Therapeutic cancer targeting peptides. *Pept Sci: Orig Res Biomol*. 2002;66(3):184-199.
21. Wu XL, Kim JH, Koo H, et al. Tumor-targeting peptide conjugated pH-responsive micelles as a potential drug carrier for cancer therapy. *Bioconjug Chem*. 2010;21(2):208-213.
22. Oh S, Kim BJ, Singh NP, Lai H, Sasaki T. Synthesis and anti-cancer activity of covalent conjugates of artemisinin and a transferrin-receptor targeting peptide. *Cancer Lett*. 2009;274(1):33-39.
23. Ellerby HM, Arap W, Ellerby LM, et al. Anti-cancer activity of targeted pro-apoptotic peptides. *Nat Med*. 1999;5(9):1032-1038.
24. Arap W, Pasqualini R, Ruoslahti E. Cancer treatment by targeted drug delivery to tumor vasculature in a mouse model. *Science*. 1998;279(5349):377-380.
25. Urbanelli L, Ronchini C, Fontana L, Menard S, Orlandi R, Monaci P. Targeted gene transduction of mammalian cells expressing the HER2/neu receptor by filamentous phage. *J Mol Biol*. 2001;313(5): 965-976.
26. Nazemian M, Hojati V, Zavareh S, Madanchi H, Hashemi-Moghaddam H. Immobilized peptide on the surface of poly l-DOPA/silica for targeted delivery of 5-fluorouracil to breast tumor. *Int J Pept Res Ther*. 2019;26(1), 259-269.
27. Khayenko V, Maric HM. Targeting GABAAR-associated proteins: new modulators. *Labels Concepts Front Mol Neurosci*. 2019;12:162.
28. Hashemi M, Dastjerdi AM, Shakerardekani A, Mirdehghan SH. Effect of alginate coating enriched with Shirazi thyme essential oil on quality of the fresh pistachio (*Pistacia vera* L.). *J Food Sci Technol-Mysore*. 2020;58, 34-43.
29. Ansari AA, Alam M, Labis JP, et al. Luminescent mesoporous LaVO₄: Eu³⁺ core-shell nanoparticles: synthesis, characterization, biocompatibility and their cytotoxicity. *J Mater Chem*. 2011;21(48):19310-19316.
30. Jiang K, Schadler LS, Siegel RW, Zhang X, Zhang H, Terrones M. Protein immobilization on carbon nanotubes via a two-step process of diimide-activated amidation. *J Mater Chem*. 2004;14(1): 37-39.
31. Vaezi M, Sadmezhaad S, Nikzad L. Electrodeposition of Ni-SiC nanocomposite coatings and evaluation of wear and corrosion resistance and electroplating characteristics. *Colloids Surf A Physicochem Eng Asp*. 2008;315(1-3):176-182.
32. Iida H, Takayanagi K, Nakanishi T, Osaka T. Synthesis of Fe₃O₄ nanoparticles with various sizes and magnetic properties by controlled hydrolysis. *J Colloid Interface Sci*. 2007;314(1):274-280.
33. Sun S, Zeng H. Size-controlled synthesis of magnetite nanoparticles. *J Am Chem Soc*. 2002;124(28):8204-8205.
34. Madanchi H, Khalaj V, Jang S, et al. AurH1: a new heptapeptide derived from Aurein1. 2 antimicrobial peptide with specific and exclusive fungicidal activity. *J Pept Sci*. 2019;25(7):e3175.
35. Zhong J, Zhao W. Novel dumbbell-like LaVO₄: Eu³⁺ nanocrystals and effect of Ba²⁺ codoping on luminescence properties of LaVO₄: Eu³⁺ nanocrystals. *J Sol-Gel Sci Technol*. 2015;73(1):133-140.
36. Judd BR. Optical absorption intensities of rare-earth ions. *Phys Rev*. 1962;127(3):750-761.
37. Ofelt G. Intensities of crystal spectra of rare-earth ions. *J Chem Phys*. 1962;37(3):511-520.
38. Yang X, Zhang Y, Zhang P, et al. pH modulations of fluorescence LaVO₄: Eu³⁺ materials with different morphologies and structures for rapidly and sensitively detecting Fe³⁺ ions. *Sens Actuators B*. 2018;267:608-616.
39. Das P, Jana NR. Dopamine functionalized polymeric nanoparticle for targeted drug delivery. *RSC Adv*. 2015;5(42):33586-33594.
40. Masoudipour E, Kashanian S, Maleki N. A targeted drug delivery system based on dopamine functionalized nano graphene oxide. *Chem Phys Lett*. 2017;668:56-63.
41. Zhang Y, Baekgaard-Laursen M, Mouritzen SA, et al. Tannic acid and cholesterol-dopamine as building blocks in composite coatings for substrate-mediated drug delivery. *Polym Int*. 2016;65(11): 1306-1314.
42. Zhang P-B, Tang A-Q, Wang Z-H, Lu J-Y, Zhu B-K, Zhu L-P. Tough poly (L-DOPA)-containing double network hydrogel beads with high capacity of dye adsorption. *Chinese J Polym Sci*. 2018;36(11):1251-1261.
43. Kumar P, Patel M, Park C, et al. Highly luminescent biocompatible CsPbBr₃@ SiO₂ core-shell nanoprobe for bioimaging and drug delivery. *J Mater Chem B*. 2020;8(45):10337-10345.
44. Mathew SA, Praveena P, Dhanavel S, Manikandan R, Senthilkumar S, Stephen A. Luminescent chitosan/carbon dots as an effective nano-drug carrier for neurodegenerative diseases. *RSC Adv*. 2020;10(41): 24386-24396.

45. Gunnlaugsson T, Gorai T, Schmitt W. Highlights of the development and application of luminescent lanthanide based coordination polymers, MOFs and functional nanomaterials. *Dalton Trans.* 2021.50(3), 770–784.
46. Chukova O, Nedilko S, Nedilko S, et al. Pulsed laser deposition of the doped lanthanum vanadate nanoparticles on glass and silicon substrates. *arXiv preprint arXiv.* 2020;2010:16259.

How to cite this article: Hashemi-Moghaddam H, Ebrahimi M, Johari B, Madanchi H. Targeted delivery of paclitaxel by NL2 peptide-functionalized on core-shell LaVO₄: Eu₃@ poly (levodopa) luminescent nanoparticles. *J Biomed Mater Res.* 2021;109:1578–1587. <https://doi.org/10.1002/jbm.b.34816>